

Impacts of particle fuelling on confinement and pedestal parameter in JT-60U

H. Takenaga¹, N. Oyama¹, H. Urano¹, K. Kamiya¹, Y. Miyo¹, T. Nishiyama¹, T. Sasajima¹, K. Masaki¹, H. Hiratsuka¹, H. Ichige¹, J. Bucalossi², E. Tsitrone², J. Gunn², C. Grisolia², A.R. Polevoi³, Y. Kamada¹ and Y. Miura¹

¹ Japan Atomic Energy Agency, 801-1 Mukouyama, Naka, Ibaraki 311-0193, Japan

² Association Euratom-CEA, CEA Cadarache, CEA-DSM-DRFC, F-13108 St Paul lez Durance, France

³ ITER International Team ITER Naka Joint Work Site, 801-1 Mukouyama, Naka, Ibaraki 311-0193, Japan

1. Introduction

In a fusion reactor, high density operation close to Greenwald density with high confinement is essential to achieve high fusion gain, where efficient and reliable fuelling system compatible with the high confinement is required. Gas-puffing is widely used due to its high reliability, but huge gas-puffing rate due to its low efficiency is concern for confinement degradation and massive tritium retention. For improving the low efficiency, supersonic molecular beam injection is used in some machines [1]. Pellet injection is considered as a fuelling method in a fusion reactor due to its high efficiency, although long pulse operation is remaining issue. High-field-side pellet injection has shown deeper deposition than low-field-side injection and compatibility with the high confinement [2]. However, large perturbation on the fusion output is expected in the case of deep penetration. It is important to investigate whether shallow pellet injection can lead the high confinement at the high density with small perturbation or not. In this paper, impacts of the shallow pellet injection on confinement and pedestal parameters in JT-60U high β_p H-mode plasmas and development of new fuelling system are discussed.

2. Fuelling system in JT-60U

JT-60U has pellet injector and gas-puffing [3] as shown in Fig. 1. The pellet injector consists of a piston type extruder and a centrifugal accelerator, which can inject (30-40) 2.1 mm cubic pellets in each discharge. The maximum injection frequency is 10 Hz and the injection speed is in the range of 100-1000 m/s. The injection lines are arranged for injections from the low-field-side midplane [LFS(mid)], the high-field-side at the top [HFS(top)] and the high-field-side midplane [HFS(mid)]. The pellet penetration depth was estimated to be $\lambda_r/a=0.1-0.3$ for the HFS(top) and HFS(mid) pellet injections from the time evolution of the electron temperature (T_e), indicating the shallow injection. This penetration depth was deeper than that predicted by the neutral gas shielding (NGS) model [4] as shown in Fig. 2 (a). On the

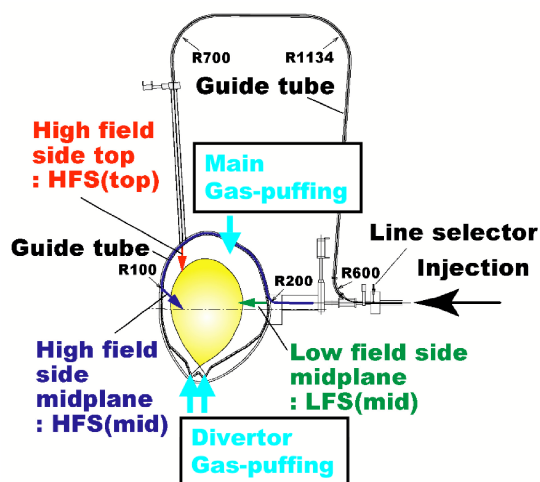


Fig. 1 Layout of fuelling system in JT-60U.

other hand, the penetration depth for the LFS(mid) injection was almost the same as the NGS model calculation. The deposition profile estimated from the density profile change before and after the pellet injection was consistent with the SMART (Simplified Mass Ablation and Relocation Treatment) prediction [5] as shown in Fig. 2 (b). In this prediction, the NGS ablation model, the initial cloud size model [6] and the mass relocation model [7] are included.

Gas-puffing is arranged at the plasma top for the main gas-puffing and below the baffle plate for the divertor gas-puffing as shown in Fig. 1. There are three ports for the main gas-puffing and two ports for the divertor gas-puffing in the toroidal direction with a set of L and H valves. The operation range is 0-3.5 Pam³/s for the L valve and 2.5-30 Pam³/s for the H valve. In this study, the main gas-puffing was used.

3. Confinement and pedestal parameter

The pellet injection was applied to high β_p H-mode plasmas with a high triangularity ($\delta > 0.3-0.5$) configuration at the plasma current of $I_p = 1$ MA and the toroidal magnetic field of $B_T = 2.0-3.6$ T, in order to extend the operation range with high confinement to high density. Figure 3 shows dependence of the confinement improvement factor over the ITER89P L-mode scaling (H_{89PL}) on the density normalized to the Greenwald density (\bar{n}_e/n_{GW}). The accessible density range with $H_{89PL} \sim 2$ was extended to $\bar{n}_e/n_{GW} \sim 0.7$ by the HFS(mid) and HFS(top) pellet injections. The penetration position of the HFS(mid) pellet injection was estimated to be $r/a = 0.77-0.84$, which is inside the ion temperature (T_i) pedestal top ($r/a = 0.86$), in the discharge with $H_{89PL} \sim 2$ at $\bar{n}_e/n_{GW} \sim 0.7$. Although the LFS(mid) pellet penetration was deeper, the density did not increase due to fast density decay ascribed to the outward drift of the ablation cloud [8]. On the other hand, the confinement degraded with gas-puffing ($H_{89PL} < 1.6$) even with the HFS(mid) pellet injection. Gas-puffed neutral particles almost ionized outside the pedestal top. The Monte-Carlo simulation using the DEGAS2 code [9] indicated that the neutral density decreases by one order of magnitude for ≤ 2 cm inside the separatrix and only 10% of the puffed neutral particle penetrates inside the T_i pedestal top at $\bar{n}_e/n_{GW} \sim 0.5$.

The profiles of n_e , T_e and T_i are shown in Fig. 4 for the HFS(mid) discharges without gas-puffing ($H_{89PL} \sim 2$ at $\bar{n}_e/n_{GW} \sim 0.7$) and with gas-puffing ($H_{89PL} \sim 1.55$ at $\bar{n}_e/n_{GW} \sim 0.75$, gas=20 Pam³/s). The density profile was almost the

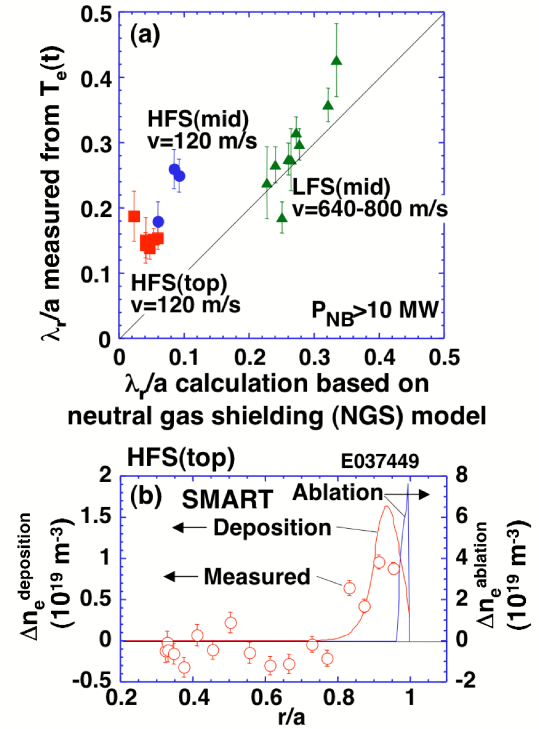


Fig. 2 (a) Comparison of the pellet penetration depth between the measurements and the NGS calculations. (b) Comparison of the pellet deposition profile between the measurements and the SMART model calculations.

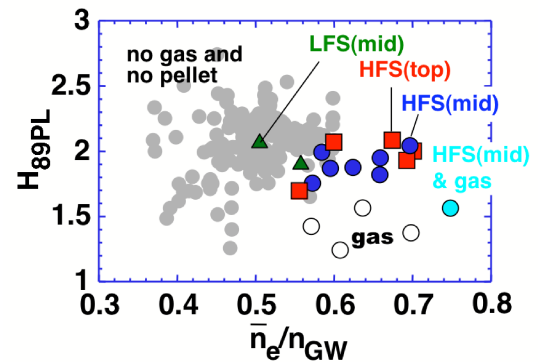


Fig. 3 H_{89PL} as a function of \bar{n}_e/n_{GW} .

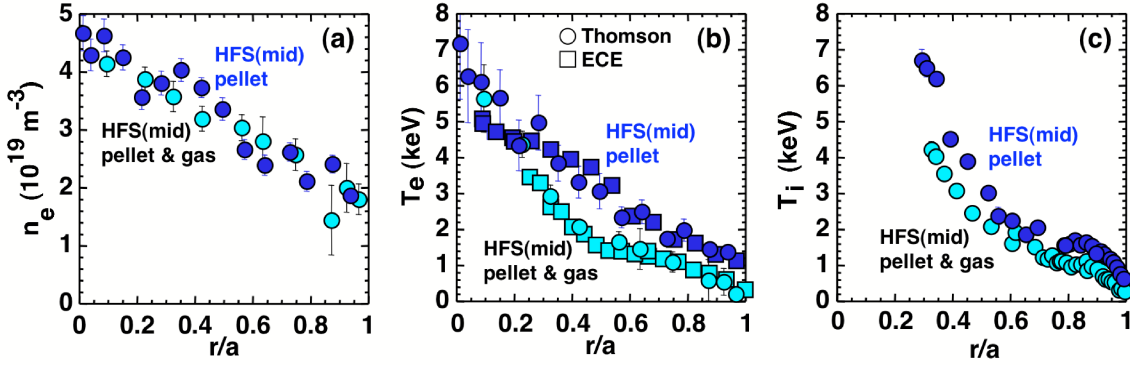


Fig. 4 Profiles of (a) electron density, (b) electron temperature and (c) ion temperature for the HFS(mid) discharges without (dark blue) and with (light blue) gas-puffing.

same for the discharges without and with gas-puffing. The values of T_e and T_i were higher without gas-puffing than with gas-puffing in the whole plasma region. The pedestal pressure was enhanced without gas-puffing, while it decreased to the same level as that in the standard ELMY H-mode plasmas as shown in Fig. 5. In JT-60U, a strong core-edge linkage has been proposed [10], where improved core confinement (high β_p) enhances the edge pressure and the enhanced edge pressure improves the core confinement. In this linkage, the confinement can be enhanced with the pedestal pressure from the stiffness level to the improved level with strong ITBs. In the T_e and T_i profiles shown in Fig. 4 (b) and (c), difference in the profiles is not clear between the discharges without and with gas-puffing. However, different time behavior was observed on T_e after the pellet injection. In the case without gas-puffing, reduction of T_e after the pellet injection was enhanced in the region of $r/a=0.39-0.53$ ($\Delta T_e(r/a=0.46)=0.35$ keV and $\Delta T_e(r/a=0.61)=0.05$ keV at $t\sim 5.8$ s) as shown in Fig. 4 (a). This time evolution indicates that the T_e profile has a structure such as ITB and this structure was affected by the shallow pellet injection. The stored energy also decreased just after the pellet injection and it recovered. Therefore, high frequency injection could lead the confinement degradation. On the other hand, cold pulse penetrated in the central region in the case with gas-puffing ($\Delta T_e(r/a=0.2-0.8)\sim 0.06-0.12$ keV) as shown in Fig. 4 (b), indicating strong stiffness. The shallow pellet injection and gas-puffing affected the core confinement/transport and the

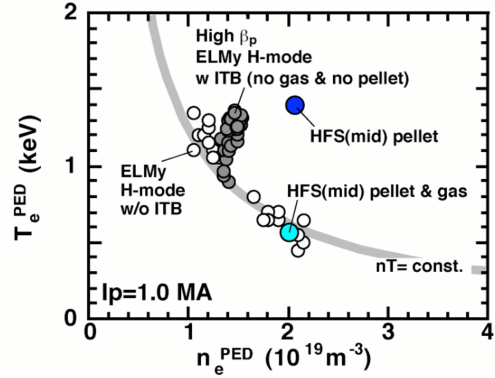


Fig. 5 nT-diagram at the pedestal top.

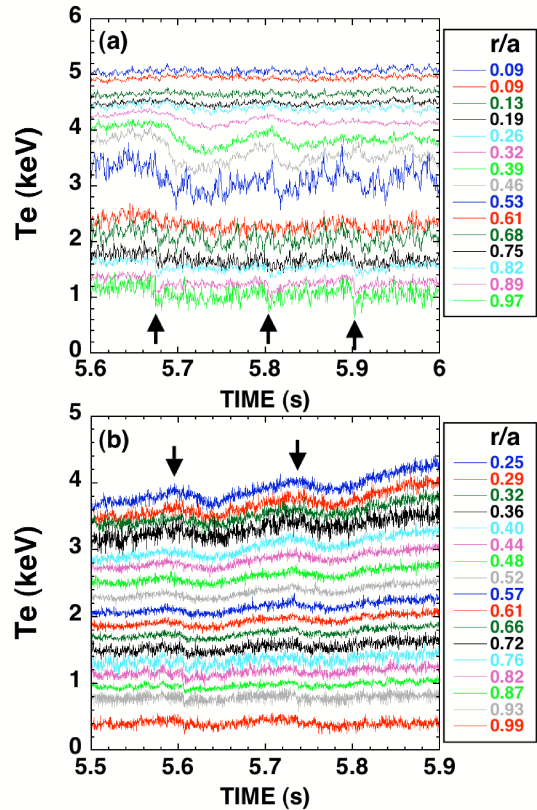


Fig. 6 T_e Time evolution after the HFS(mid) pellet injections (arrows) in the discharges (a) without and (b) with gas-puffing.

structure formation such as ITB through the strong core-edge linkage. The shallow pellet injection was compatible with the high confinement at high density. However, the perturbation was induced in the core region. It should be clarified whether this perturbation is acceptable or not in future work.

4. Development of new fuelling system

In order to further extend the operation regime to high density and to investigate impacts of high frequency pellet injection on confinement and pedestal parameter, the pellet injector is being modified for longer duration (from 5-6 s to ~60 s) and higher frequency (from ≤ 10 Hz to ≤ 20 Hz) using the screw type pellet extruder (PELIN Laboratory). The screw type pellet extruder can produce 2.1 mm x 2.1 mm ice rod with 46 mm/s (~20 Hz injection) for 60 s and 38 mm/s for 360 s. The screw type pellet extruder was assembled with the centrifugal accelerator. The production of good quality ice rod has been confirmed in some operation conditions. The liquefier and nozzle temperatures are being optimized. Also, supersonic molecular beam injector (SMBI) was installed both on HFS and LFS in collaboration with CEA Cadarache. The injector head is the same as that installed in Tore Supra [1]. The SMBI can be operated with a frequency of 8-10 Hz and 2 ms duration per pulse. Theoretical gas flow was evaluated to be $510 \text{ Pam}^3/\text{s}$ (amount of the injected gas was $Q_{\text{gas}} \sim 1 \text{ Pam}^3$ per pulse) with a mach number of 4.1 (speed of 2.2 km/s) at operation temperature of $T=150^\circ\text{C}$ and background pressure of $P_{\text{BK}}=5$ bar. A deeper fuelling is expected compared with the gas-puffing and a shallower fuelling is expected compared with the pellet injection. Gas injection test was performed using He gas at $T=150^\circ\text{C}$ and $P_{\text{BK}}=2$ bar. The value of Q_{gas} was estimated to be 0.14 Pam^3 , which could be decreased due to T-junction for switching the HFS and LFS injector heads.

5. Summary

High confinement of $H_{89\text{PL}} \sim 2$ was achieved at $\bar{n}_e/n_{\text{GW}}=0.7$ with the HFS shallow pellet injections. Pellet injection and gas-puffing affected confinement, core transport and structure formation such as ITB through the strong core-edge linkage. New fuelling system is being developed using the screw type pellet extruder for long operation and high frequency, and the SMBI in collaboration with CEA-Cadarache.

Acknowledgement

This work was partly supported by JSPS, Grant-in-Aid for Scientific Research (A) No. 16206093 and (B) No. 17360447.

References

- [1] J. Bucalossi et al., Proc. 19th IAEA Fusion Energy Conf. (Lyon, 2002) EX/P4-04.
- [2] P. T. Lang et al., Plasma Phys. Control. Fusion **44**, 1919 (2002).
- [3] K. Kizu, et al., Fusion Science and Technology, **42**, 396 (2002).
- [4] B. Kuteev, Nucl. Fusion **35**, 431 (1995).
- [5] A. Polevoi et al., Plasma Phys. Control. Fusion, **43**, 1525 (2001).
- [6] P. B. Parks, et al., Phys. Plasmas **7**, 1968 (2000).
- [7] H. R. Strauss and W. Park, Phys. of plasmas **5**, 2676 (1998).
- [8] H. Takenaga and the JT-60 Team, Phys. Plasmas, **8**, 2217 (2001).
- [9] D. P. Stotler and C. F. F. Karney, Contrib. Plasma Phys. **34**, 392 (1994).
- [10] Y. Kamada et al., Plasma Phys. Control. Fusion, **44**, A279 (2002).